Engineering Computations

A poly-ellipsoid particle for non-spherical discrete element method

John F. Peters Mark A. Hopkins Raju Kala Ronald E. Wahl

Article information:

To cite this document:
John F. Peters Mark A. Hopkins Raju Kala Ronald E. Wahl, (2009),"A poly#ellipsoid particle for non#spherical discrete element method", Engineering Computations, Vol. 26 Iss 6 pp. 645 - 657
Permanent link to this document:
http://dx.doi.org/10.1108/02644400910975441

A poly-ellipsoid particle for non-spherical discrete element method

John F. Peters, Mark A. Hopkins, Raju Kala
and Ronald E. Wahl
US Army Engineer Research and Development Center, Vicksburg, Mississippi, USA

Abstract

Purpose – The purpose of this paper is to present a simple non-symmetric shape, the poly-ellipsoid, to describe particles in discrete element simulations that incur a computational cost similar to ellipsoidal particles.

Design/methodology/approach – Particle shapes are derived from joining octants of eight ellipsoids, each having different aspect ratios, across their respective principal planes to produce a compound surface that is continuous in both surface coordinate and normal direction. Because each octant of the poly-ellipsoid is described as an ellipsoid, the mathematical representation of the particle shape can be in the form of either an implicit function or as parametric equations.

Findings – The particle surface is defined by six parameters (vs the 24 parameters required to define the eight component ellipsoids) owing to dependencies among parameters that must be imposed to create continuous intersections. Despite the complexity of the particle shapes, the particle mass, centroid and moment of inertia tensor can all be computed in closed form.

Practical implications – The particle can be implemented in any contact algorithm designed for ellipsoids with minor modifications to determine in which pair of octants the potential contact occurs.

Originality/value – The poly-ellipsoid particle is a computational device to represent non-spherical particles in DEM models.

Keywords Geometric planes and solids, Particle size measurement, Programming languages

Paper type Research paper

Introduction

The discrete element method (DEM) (Cundall and Strack, 1979) provides a means to perform numerical simulations of granular systems, thus providing access to details of particle motion and contact forces not available from physical experiments alone. The use of DEM and physical experiments in tandem provides engineers and physicists a new view of how granular media behave, which has led to a deeper understanding of granular mechanics. DEM simulations can now be used to model very large-scale particle systems in three dimensions under realistic boundary conditions such that capabilities now extend beyond the study of simple academic problems. However, the accuracy of large-scale simulations is still limited by the practical necessity of representing particles as simple shapes, usually spheres, which can greatly bias the conclusions made from simulation-based studies. In particular, the role of particle rotations vs inter-particle sliding is greatly exaggerated for spherical particles because rotations can occur within the volume of the particle. For irregular particle shapes,

This work was supported by the Engineer Research and Development Center's basic research project entitled "Stress Transfer in Granular Media". Permission to publish this information is given by the Director of the Geotechnical and Structures Laboratory of the ERDC.

Engineering Computations: International Journal for Computer-Aided Engineering and Software
Vol. 26 No. 6, 2009
pp. 645-657

0264-4401
DOI 10.1108/02644400910975441

rotations necessarily require volumetric changes to occur within the assemblage. Thus, assemblages of spherical particles tend to become unstable because particles can seek more stable configurations without incurring the energy cost of dilating the assemblage. Further, the instability of particle groups in spherical assemblies tend to evolve from buckling motions, again because of the ability of spherical particles to rotate. As a result, many simulation-based studies of granular media overemphasize the effects of rotations and buckling in description of particle kinematics.

In fact, there are two motivations for using DEM: prototype-scale simulations for engineering studies and micromechanical studies for study of fundamental mechanics. For prototype-scale computations, the DEM is used similarly to the finite element method to capture large-scale non-continuous motions (e.g. Horner *et al.*, 2001). Prototype scale analyses require accurate bulk behavior of the medium, which presumably can be achieved without capturing details at the particle scale. In fact, in such studies both particle size and shape are sacrificed to obtain problem sizes suitable for practical computations. For micromechanical studies, greater fidelity to the actual particle characteristics is needed, because for simulation to be on equal footing with physical experiments, the particle-scale behavior must be correct. Simply reproducing bulk behavior is not sufficient if the intent is to develop generalizations about fundamental mechanics.

One approach to limiting rotations is to use compound particles composed of clusters of spherical particles that rotate as non-spherical rigid bodies about common centers of mass (e.g. Favier *et al.*, 2001; Lu and McDowell, 2007). The advantage to the cluster particle approach is that the numerical procedure for contact detection is nearly unaltered. The disadvantage is that particle shape is only approximated. Other non-spherical shapes such as ellipsoids and hyper-ellipsoids have been used to extend the particle representation (e.g. Cleary *et al.*, 1997; Kuhn, 2002). The computational costs for such shapes are greater than simple spherical particles, but it has been demonstrated that simulations of sufficient size can be performed to be of practical use. In all cases, the motivation of the non-spherical particle is to achieve more realistic particle rotations and allow bulk properties to be represented.

Resistance to rotation can be implemented directly into the contact laws (Tordesillas and Walsh, 2002), without incurring significant loss in computational efficiency. Inter-particle rolling resistance produces much more realistic bulk behavior for prototype analyses but does not necessarily address all aspects of the micromechanics of real particles. When non-physical rolling resistance is added to contact laws, chains of spherical particles become beam-column structures that can be analyzed by elastic buckling theory. As noted previously, particle-scale analyses based on such non-physical contact mechanisms become skewed toward kinematic models that are atypical of actual granular media.

In principle, particle shape is not a limitation to the DEM method. Nezami *et al.* (2004) constructed complex shapes from polyhedra based on measurements of real particles. Such shapes have been used in simulations of sufficient size to be practical for modeling materials handling systems such as scoops and loaders. At issue is the ability to model particles in sufficient numbers to recreate granular media that can be studied as a continua. The practicality of such simulations has two components. First, simulations with non-spherical particles require a greater computation time for contact detection than spherical particles. Second, the number of parameters needed to describe the geometry of each particle increases as the particle shape deviates from a sphere. What is needed is a particle shape that is amenable to efficient contact detection algorithms, has a low parameterization overhead and yet is reasonably representative of a wider range of granular media.

This paper presents a simple non-symmetric shape that incurs a computational cost similar to elliptical particles. The shapes are smooth, and thus suitable for modeling pebble-like particles. However, the shapes can be quite non-symmetric providing a greater range in representing realistic assemblies in which sphericity, aspect ratio, and to some extent, angularity can be varied. In the discussion section, extensions of the method to more angular shapes are considered.

Particle geometry

The method of creating particle shapes is based on the observation that ellipsoids having different aspect ratios can be joined along their respective principal planes to produce a compound particle with a surface that is continuous in both surface coordinate and normal direction. In Figure 1, a compound shape is created by joining octants from eight different ellipsoids. Accordingly, such shapes will be referred to as poly-ellipsoids. Each octant of a "unit" ellipsoid centered at (x_o, y_o, z_o) can be described as an implicit function

$$a(x-x_o)^2 + b(y-y_o)^2 + c(z-z_o)^2 - 1 = 0 \tag{1}$$

where the principal axes of the ellipsoid correspond with the coordinate axes (x, y, z) and the parameters a, b, and c control the elongation of shape along each principal direction. Alternatively, the parametric form in spherical coordinates (Figure 2) can be used

$$\begin{aligned} x - x_o &= R\alpha \sin\theta \sin\phi, \\ y - y_o &= R\beta \cos\theta \sin\phi, \\ z - z_o &= R\gamma \cos\phi. \end{aligned} \tag{2}$$

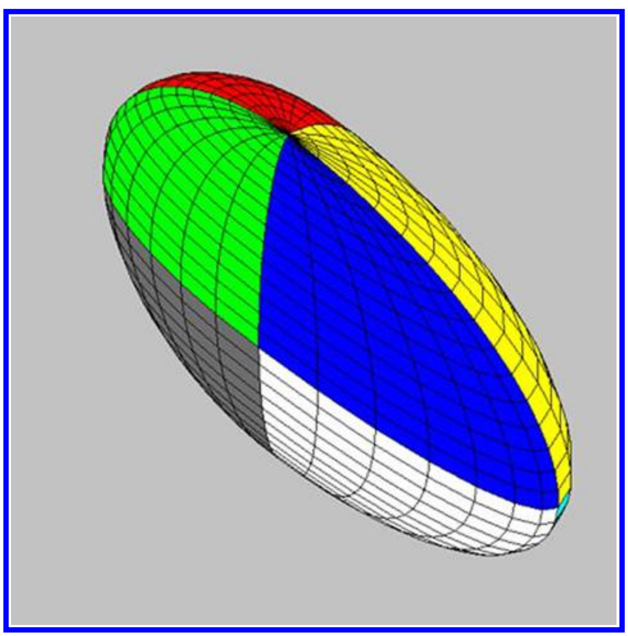

Figure 1.
Particle created by combining the octants of eight ellipsoids

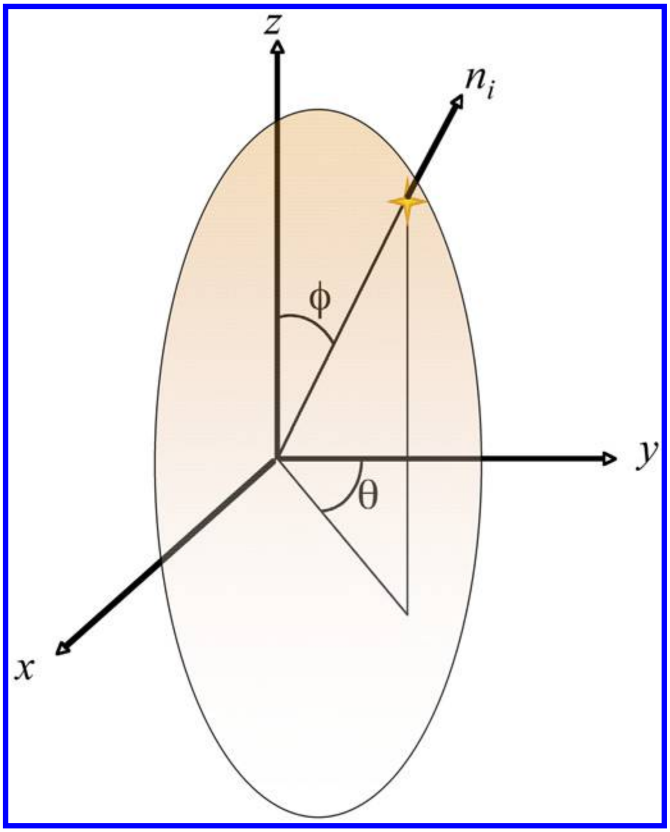

Figure 2.
Surface showing both Cartesian and spherical coordinates

Where $\alpha = 1/\sqrt{a}$, $\beta = 1/\sqrt{b}$, and $\gamma = 1/\sqrt{c}$ are dimensionless and the parameter R has been included to control particle size. Thus, the shape of the ellipsoid component is defined by three parameters. To this must be added three parameters that define the orientation of the principal axes. The particle surface of the poly-ellipsoid is defined by six parameters rather than the 24 parameters that define the eight component ellipsoids owing to dependencies among parameters that must be imposed to create continuous surfaces at intersections across the principal planes. For example, the ellipsoids that join in octants 1 and 2 are given by the equation pair

$$a_1(x - x_o)^2 + b_1(y - y_o)^2 + c_1(z - z_o)^2 - 1 = 0 \tag{3}$$

and

$$a_2(x - x_o)^2 + b_2(y - y_o)^2 + c_2(z - z_o)^2 - 1 = 0 \tag{4}$$

With reference to the parametric form of the equations, at this intersection, $\theta = 0$ and the coordinates y and z must be equal for all ϕ. Thus, $\beta_1 = \beta_2$ and $\gamma_1 = \gamma_2$. Similar relationships can be made for the boundaries shared by each pair of octants, yielding six independent parameters as follows:

$$\begin{aligned} \alpha_2 = \alpha_3 = \alpha_6 = \alpha_7 &= \alpha^+ \\ \alpha_1 = \alpha_4 = \alpha_5 = \alpha_8 &= \alpha^- \\ \beta_1 = \beta_2 = \beta_5 = \beta_6 &= \beta^+ \\ \beta_3 = \beta_4 = \beta_7 = \beta_8 &= \beta^- \\ \gamma_1 = \gamma_2 = \gamma_3 = \gamma_4 &= \gamma^+ \\ \gamma_5 = \gamma_6 = \gamma_7 = \gamma_8 &= \gamma^- \end{aligned}$$

An alternative interpretation of the particle shape is that of an ellipsoid for which different elongations are used in the positive and negative directions of each principal axes giving the parameter set (α^+, β^+, γ^+, α^-, β^-, γ^-). All eight ellipsoid components share the same principal axes, requiring three parameters to define the orientation of the particle in space.

The range in shapes that can be captured by the poly-ellipsoid is quite broad as illustrated in Figure 3. The sphere and ellipsoid, of course, can be modeled exactly. However, elongated, flattened, rod-like shapes are also possible. Thus, this class of particle gives a good approximation to well-rounded aggregates derived from stream-deposited materials, as illustrated by the particles in Figure 4 obtained by randomly perturbing the six shape parameters.

Particle properties

Despite the complexity of the particle shapes, the particle mass, centroid, and moment of inertia tensor can all be computed in closed form. Consider the case of an octant of an ellipsoid in which the principal axes are aligned with the coordinate axes with

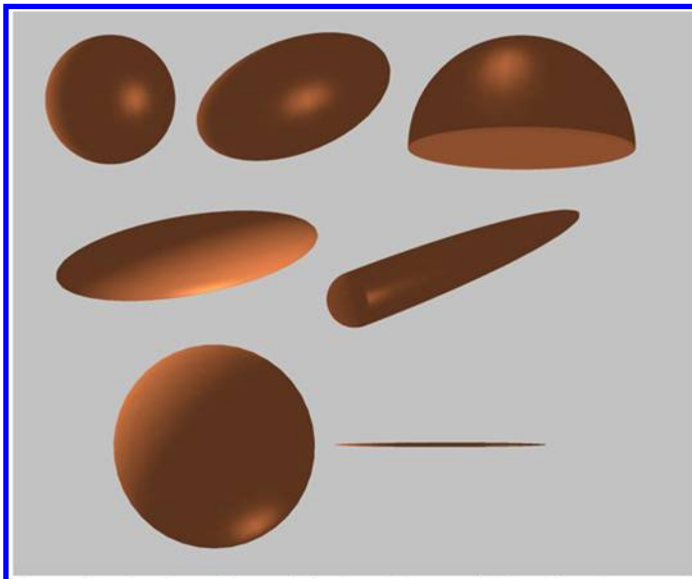

Notes: Starting from the top left, these shapes will be referred to as sphere, egg, half-dome, ellipsoid, carrot, and disc (both side and edge views shown)

Figure 3. Samples of particles created from poly-ellipsoid shapes

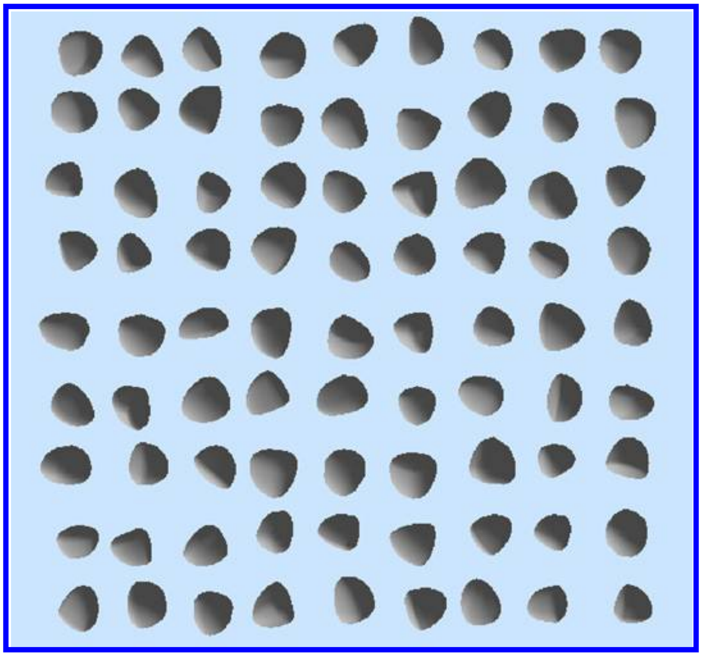

Figure 4.
Pebble-like shapes

parametric parameters (α, β, γ). Using a procedure similar to Weisstein (2007) the following can be readily obtained for each octant (see Appendix):

Volume and mass.

$$V = \alpha\beta\gamma\frac{\pi}{6}R^3 \tag{5}$$

$$M = \rho V \tag{6}$$

Centroid.

$$\bar{x} = \frac{3}{8}\alpha R, \qquad \bar{y} = \frac{3}{8}\beta R, \qquad \bar{z} = \frac{3}{8}\gamma R \tag{7}$$

Moment of inertia.

$$\mathbf{I} = \frac{R^2 M}{5\pi}\begin{bmatrix} (\beta^2+\gamma^2)\pi & \pm 2\alpha\beta & \pm 2\alpha\gamma \\ \pm 2\alpha\beta & (\alpha^2+\gamma^2)\pi & \pm 2\beta\gamma \\ \pm 2\alpha\gamma & \pm 2\beta\gamma & (\alpha^2+\beta^2)\pi \end{bmatrix} \tag{8}$$

where ρ is the mass density and the sign of the off-diagonal terms in Equation (8) depend on the octant; the sign is positive for odd numbered octants and negative for even numbered octants.

These quantities are all computed relative to the center of geometry (see Figure 5). For integration of the equations of motion, the centroid and moment of

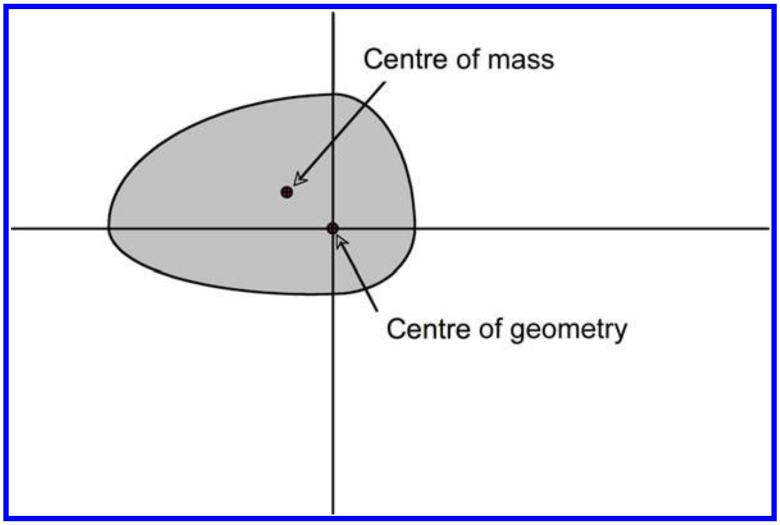

Figure 5.
Comparison of center of geometry to center of mass

inertia tensors must be known for the poly-ellipsoid relative to the center of mass as given by

$$\bar{x}_c = \frac{\sum_{i=1}^{8} M_i \bar{x}_i}{\sum_{i=1}^{8} M_i}, \qquad \bar{y}_c = \frac{\sum_{i=1}^{8} M_i \bar{y}_i}{\sum_{i=1}^{8} M_i}, \qquad \bar{z}_c = \frac{\sum_{i=1}^{8} M_i \bar{z}_i}{\sum_{i=1}^{8} M_i} \tag{9}$$

The composite moment of inertia about the axes of geometry are found by simple summation of the octant quantities, whereby for example

$$I^c_{xx} = \sum_{i=1}^{8} I^i_{xx}, \tag{10}$$

which can be used to compute the moments of inertial using the parallel axis theorem whereby for example, the diagonal term is given by

$$I_{\bar{x}\bar{x}} = \sum_{c=1}^{8} (I^c_{xx} + \bar{x}^2_c M_c) \tag{11}$$

and for an off-diagonal term

$$I_{\bar{x}\bar{y}} = \sum_{c=1}^{8} (I^c_{xy} + \bar{x}_c \bar{y}_c M_c) = I_{\bar{y}\bar{x}} \tag{12}$$

The normal to the surface defined by $F = a(x - x_o)^2 + b(y - y_o)^2 + c(z - z_o)^2 - 1$ is

$$\nabla F = \begin{Bmatrix} \dfrac{\partial F}{\partial x} \\ \dfrac{\partial F}{\partial y} \\ \dfrac{\partial F}{\partial z} \end{Bmatrix} = 2 \begin{Bmatrix} a(x - x_o) \\ b(y - y_o) \\ c(z - z_o) \end{Bmatrix} \tag{13}$$

For contact detection algorithms based on Newton–Raphson iteration (e.g. Cleary *et al.*, 1997), the gradient of the surface normal vector is also required. For an ellipsoid, this gradient matrix is constant. Thus, for each octant,

$$\nabla^2 F = 2 \begin{bmatrix} a & 0 & 0 \\ 0 & b & 0 \\ 0 & 0 & c \end{bmatrix} \tag{14}$$

Note that the matrix is diagonal because the coordinate axes are aligned with the principal axes of the particle.

Remarks on implementation

The most expensive part of any DEM computation is contact detection. The simplest case for contact detection is the sphere-on-sphere contact, although relatively inexpensive contact detection has been developed for ellipsoids and other axially symmetric solids. The advantage of the poly-ellipsoid is that any method that is suited for ellipsoids can be readily modified for poly-ellipsoids by an additional check to determine the octant in which a potential contact point sits. The formulas given in the preceding section are simple because it was assumed the principal axes of the particle coincides with the global coordinate directions. It is therefore convenient to define a local particle coordinate system that is alligned with the principal axes of the particle. The potential contact point in global coordinates, $\mathbf{x}_c^g$, is transformed to the local particle coordinate, $\mathbf{x}_c^p$, through a rotation given the geometric center in global coordinates, $\mathbf{x}_o^g$ and the rotation matrix $\mathbf{R}$,

$$\mathbf{x}_c^p = \mathbf{R}(\mathbf{x}_c^g - \mathbf{x}_o^g). \tag{15}$$

Note that because particle coordinates are referenced to the geometric center, $\mathbf{x}_c^p = 0$. The particle shape parameters that apply to the point can thus be determined using the following criteria:

$$\begin{array}{llll} x_c^p > 0, & \alpha = \alpha^+ & \text{else} & \alpha = \alpha^- \\ y_c^p > 0, & \beta = \beta^+ & \text{else} & \beta = \beta^- \\ z_c^p > 0, & \gamma = \gamma^+ & \text{else} & \gamma = \gamma^- \end{array}$$

The direction of the normal vector and its gradient in global coordinates are given as follows:

$$(\nabla F)^g = \mathbf{R}^T (\nabla F)^p \tag{16}$$

and

$$(\nabla^2 F)^g = \mathbf{R}^T (\nabla F)^p \mathbf{R}. \tag{17}$$

Example computations

The simulations of a cyclic load triaxial test were performed on problems with 1,700 particles (see Figure 6). The code is written for parallel computations and the total number of particles can be increased to several hundred thousand particles depending on the number of processors available. The simulations involved interactions between particles, particles and platten, membrane, and platten and particles and membrane. Two iterative contact detection approaches were used based on the algorithm of Hopkins (2004) and the Newton–Raphson procedure of Cleary *et al.* (1997). As reported by Cleary *et al.* (1997) the Newton–Raphson iteration was slower for contacts with small radius of curvature. Particles with sharp edges, such as the half-dome shape, were found to be especially troubling. After some modification, the Hopkins algorithm gave reliable contact detection for all particles while the Newton–Raphson procedure generally failed to converge when the contact point fell on a sharp edge.

Discussion

The poly-ellipsoid is best suited for smooth particles found in beach and river deposits. Although real particle shapes cannot be modeled exactly, the particles can be parameterized by fitting to common descriptive measures such as aspect ratio and sphericity (ratio of the surface area of a sphere having the same volume as the particle to the surface area of the particle). As for spheres, the size of the particles can be varied to fit some predetermined size-gradation curve. To reduce storage requirements for large-scale simulations, the α, β and γ parameters for a few hundred equally likely shapes can be given unique identifiers. The particle description then requires only a shape identifier and size.

The smoothness of the poly-ellipsoid particles is still a limiting factor in modeling the full range of particles found in natural materials. These shapes are suited best for rounded materials common to river deposits. Contacts are necessarily between smooth surfaces. Materials derived from crushed stone are angular whereby contacts typically are edge to face. While contact behavior can be parameterized to account for features such as surface roughness and local curvature, the practical difficulty in defining the requisite parameters for angularity makes such an approach unattractive for fundamental studies. Further, the tendency for particles to pack is controlled by angularity as well as shape. Therefore, an efficient procedure for modeling angular materials is still of interest.

As noted in the introduction, the problem in this case is the compactness of parameterization; angular particles must be modeled by polygonal faces, which necessarily require a large numerical overhead to store the location of vertices. A possible alternative is to project the poly-ellipsoid on a regular faceted mesh; the poly-ellipsoid captures the shape of the particle and the faceted mesh captures the angularity. Each particle is still described by six parameters. In this scheme, the faceted mesh is common to all particles, thus the overhead for storage is minimal. For example, poly-ellipsoid coordinates can be projected onto a mesh of a sphere, as shown in Figure 7, to produce an angular particle. The angle pair (θ, ϕ) can be computed for each vertex in the mesh. The radius can be computed from the parametric form of the poly-ellipsoid equations. The coarseness of the finite element representation of the sphere controls the angularity of the particle. Contact detection algorithms suitable for polyhedra can be used (e.g. Nezami *et al.*, 2004).

Another deficiency of the poly-ellipsoids and their various derivatives is that only convex particles are represented. The convexity property restricts the physical

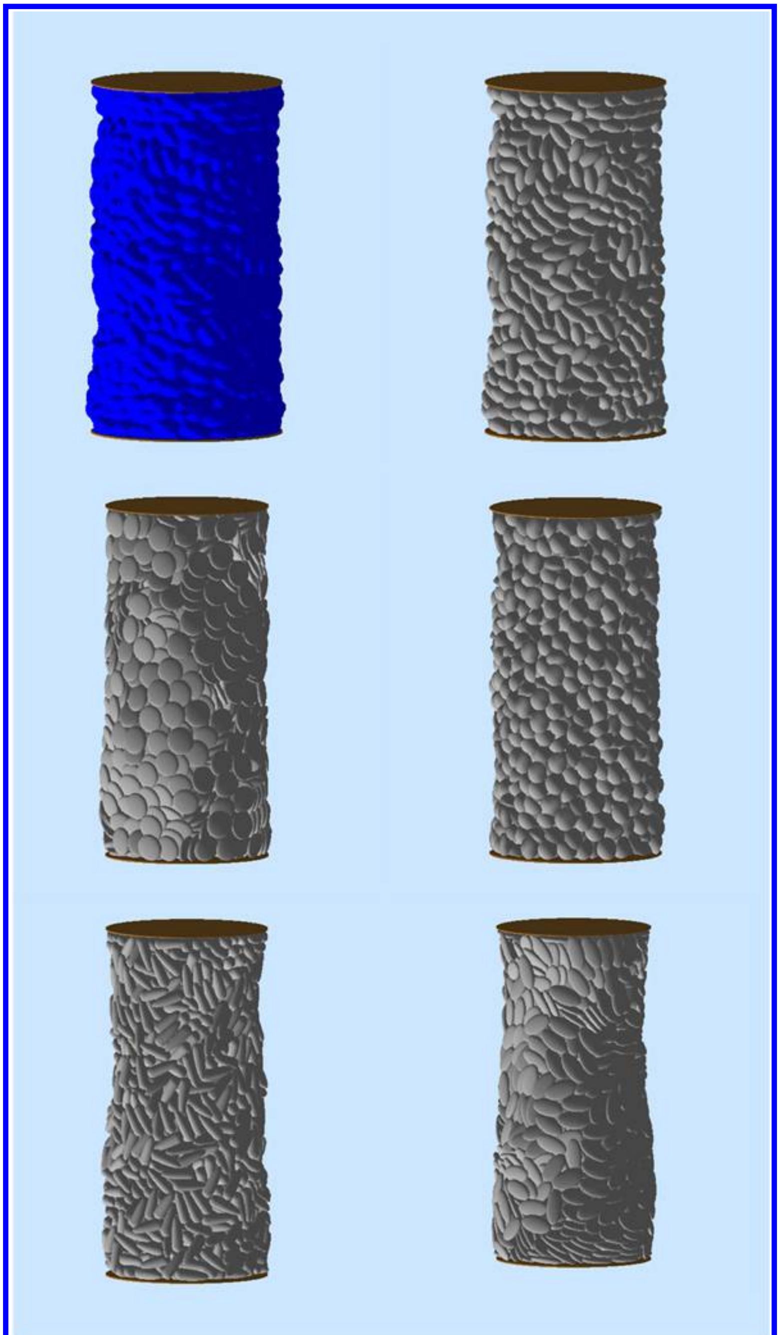

Notes: A triaxial specimen with membrane is shown in the upper left-hand corner. Continuing clockwise are eggs, half-domes, ellipsoids, carrots, and discs

Source: Details of simulations to appear in Uthus *et al*. (2008)

Figure 6.
Specimens used for triaxial compression test simulations

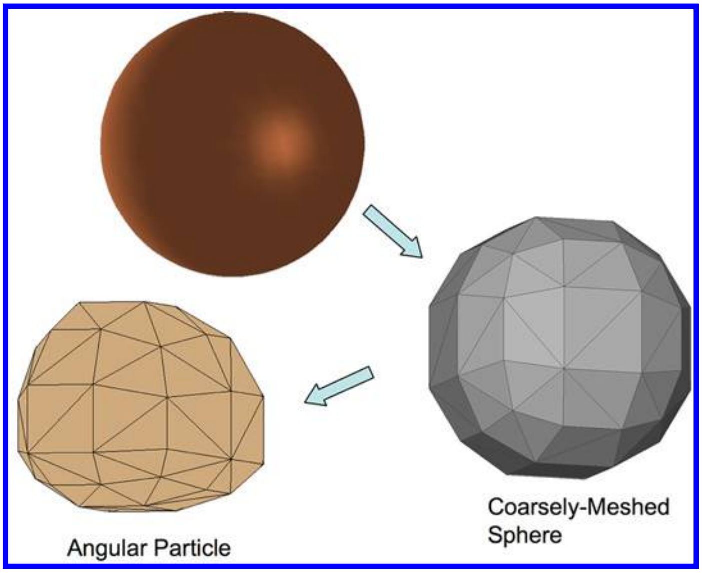

Figure 7.
Angular particle created by projecting a poly-ellipsoid shape onto a coarse mesh of a sphere

interaction of particles because it precludes multiple contacts between particle pairs. Non-convex particle shapes are common in real granular materials and need to be included in any comprehensive DEM capability. To achieve this capability, considerable work in needed in particle representation and parameterization as well as contact detection.

Conclusions

Micromechanical studies of granular media via the DEM are hampered by the practical limitation of using spherical shapes in large-scale computations. The poly-ellipsoid provides an avenue for studies of granular materials having non-spherical particle shapes. Implementation of these particle shapes is similar to that of an ellipsoid particle. While more computationally expensive than spheres or spherical clusters, use of poly-ellipsoids is still practical for large particle assemblages. Even though smooth particle surfaces with sharp edges can be created, contact detection was found to be a problem for some shapes. Particles with sharp edges, such as the half-dome shape used in the example computations, posed difficulties for the Newton–Raphson algorithm. Reliable contact detection was achieved for the algorithm of Hopkins (2004).

References

Cleary, P.W., Stokes, N. and Hurley, J. (1997), “Efficient collision detection for three dimensional super-ellipsoidal particles”, *Proceedings of the CTAC97*, University of Adelaide, Adelaide.

Cundall, P.A. and Strack, O.D.L. (1979), “A distinct element model for granular assemblies”, *Geotechnique*, Vol. 29, pp. 47-65.

Favier, J.F., Abbaspour-Fard, M.H., and Dremmer, M. (2001), “Modeling nonspherical particles using multisphere discrete elements”, *ASCE Journal of Engineering Mechanics*, Vol. 127 No. 10, pp. 971-77.

Hopkins, M.A. (2004), “Discrete element modeling with dilated particles”, *Engineering Computations*, Vol. 21 Nos 2-4, pp. 422-30.

Horner, D.A., Peters, J.F. and Carrillo, A. (2001), "Large scale discrete element modeling of vehicle-soil interaction", *ASCE Journal of Engineering Mechanics*, Vol. 127 No. 10, pp. 1027-32.

Kuhn, M.R. (2002), "Smooth convex three-dimensional particle for the discrete-element method", *ASCE Journal of Engineering Mechanics*, Vol. 129 No. 5, pp. 539-47.

Lu, M. and McDowell, G.R. (2007), "The importance of modelling ballast particle shape in the discrete element method", *Granular Matter*, Vol. 9 Nos 1-2, pp. 69-80.

Nezami, E., Hashash, Y.M.A., Zhao, D. and Ghaboussi, J. (2004), "A fast contact detection algorithm for 3D discrete element method", *Computers and Geotechnics*, Vol. 31, pp. 575-87.

Tordesillas, A. and Walsh, S.D.C. (2002), "Incorporating rolling resistance and contact anisotropy in micromechanical models of granular media", *Powder Technology*, Vol. 124, pp. 106-11.

Uthus, L., Hopkins, M.A. and Horvli, I. (2008), "Discrete element modeling of the resilient behavior of unbound granular aggregates", *International Journal of Pavement Engineering*, (forthcoming).

Weisstein, E. (2007), "Moment of inertia–ellipsoid", *Wolfram Research Science World*, available at: http://scienceworld.wolfram.com/physics/MomentofInertiaEllipsoid.html

Appendix

The computation of volumetric integrals is illustrated for the moment of inertia for an ellipsoid by Weisstein (2007). First consider the volume of an ellipsoid defined by

$$V = \int_{V_e} dx\, dy\, dz, \tag{18}$$

where V_e is the domain of the ellipsoid. The domain can be transformed to that of a sphere having radius R using the transformation

$$x' = x/\alpha, \qquad y' = y/\beta, \qquad z' = z/\gamma \tag{19}$$

by which the integral becomes

$$V = \int_{V_s} (\alpha x')(\beta y') J\, dx'\, dy'\, dz', \tag{20}$$

where V_s refers to the domain of the sphere and J is the Jacobian of transformation given by

$$J = \left| \frac{\partial[xyz]}{\partial[x'y'z']} \right| = \alpha\beta\gamma. \tag{21}$$

The integral becomes

$$V = \rho \int_{V_s} J\, dx'\, dy'\, dz'. \tag{22}$$

Evaluation of the integral is simplified by adopting spherical coordinates

$$x' = r \cos\theta \sin\phi, \qquad y' = r \sin\theta \sin\phi, \qquad z' = r \cos\phi. \tag{23}$$

with

$$dx'\, dy'\, dz' = r^2 \sin\phi\, d\phi\, d\theta\, dr \tag{24}$$

The integral now becomes

$$V = \alpha\beta\gamma \int_0^R \int_0^{\pi/2} \int_0^{\pi/2} r^2 \sin\ \phi\, d\phi\, d\theta\, dr$$
$$= \alpha\beta\gamma \frac{\pi R^3}{6} \tag{25}$$

The limit of integration for θ and ϕ corresponds to the octant 1 of the ellipsoid. Note that the integral is equal and positive and for all octants and that for $\alpha = \beta = \gamma = 1$, summation of all eight quadrants gives the volume of a sphere, $4\pi R^3/3$.

The definition of I_{xy} is given by

$$I_{xy} = \rho \int_{V_e} xy\, dx\, dy\, dz. \tag{26}$$

After conversion to integration on the sphere, the integral becomes

$$I_{xy} = \rho\alpha\beta\gamma \int_0^R \int_0^{\pi/2} \int_0^{\pi/2} (r\alpha\ \cos\theta\ \sin\phi)(r\beta\ \sin\theta\ \sin\phi)\, r^2\, d\phi\, d\theta\, dr$$
$$= \frac{2\alpha\beta R^2 M}{5\pi}. \tag{27}$$

Note that the sign of the integral depends on the octant for which the integral is computed. Integrals for I_{xz} and I_{yz} can be similarly derived by permuting x, y and z, as can the symmetry conditions $I_{xy} = I_{yx}$, $I_{xz} = I_{zx}$, and $I_{zy} = I_{yz}$.

Corresponding author
John F. Peters can be contacted at: john.f.peters@usace.army.mil

This article has been cited by:

1. Bart Smeets, Tim Odenthal, Janos Keresztes, Simon Vanmaercke, Paul Van Liedekerke, Engelbert Tijskens, Wouter Saeys, Hans Van Oosterwyck, Herman Ramon. 2014. Modeling contact interactions between triangulated rounded bodies for the discrete element method. *Computer Methods in Applied Mechanics and Engineering* **277**, 219-238. [CrossRef]
2. Gang Ma, Wei Zhou, Xiao-Lin Chang, Wei Yuan. 2014. Combined FEM/DEM Modeling of Triaxial Compression Tests for Rockfills with Polyhedral Particles. *International Journal of Geomechanics* **14**, 04014014. [CrossRef]
3. Qin Fang, Jinhua Zhang, Li Chen, Jinchun Liu, Junyu Fan, Yadong Zhang. 2014. An algorithm for the grain-level modelling of a dry sand particulate system. *Modelling and Simulation in Materials Science and Engineering* **22**:5, 055021. [CrossRef]
4. Mingjing Jiang, Fang Liu, Zhifu Shen, Min Zheng. 2014. Distinct element simulation of lugged wheel performance under extraterrestrial environmental effects. *Acta Astronautica* **99**, 37-51. [CrossRef]
5. Mark A. Hopkins. 2014. Polyhedra faster than spheres?. *Engineering Computations* **31**:3, 567-583. [Abstract] [Full Text] [PDF]
6. Antoinette Tordesillas, Sebastian Pucilowski, David M. Walker, John F. Peters, Laura E. Walizer. 2014. Micromechanics of vortices in granular media: connection to shear bands and implications for continuum modelling of failure in geomaterials. *International Journal for Numerical and Analytical Methods in Geomechanics* n/a-n/a. [CrossRef]
7. S.R. Buechler, S.M. Johnson. 2013. Efficient generation of densely packed convex polyhedra for 3D discrete and finite-discrete element methods. *International Journal for Numerical Methods in Engineering* **94**:1, 1-19. [CrossRef]
8. M.A. Knuth, J.B. Johnson, M.A. Hopkins, R.J. Sullivan, J.M. Moore. 2012. Discrete element modeling of a Mars Exploration Rover wheel in granular material. *Journal of Terramechanics* **49**:1, 27-36. [CrossRef]
9. S.A. Galindo-Torres, D.M. Pedroso, D.J. Williams, L. Li. 2012. Breaking processes in three-dimensional bonded granular materials with general shapes. *Computer Physics Communications* **183**:2, 266-277. [CrossRef]
10. Methods of Mechanics of Discontinua 21-38. [CrossRef]